ANALYSIS OF INTRAPULSE CHIRP IN CO_2 OSCILLATORS

Stephen E. Moody, Russell G. Berger, and William J. Thayer III
Spectra Technology, Inc.
Bellevue, Washington

SUMMARY

Pulsed single-frequency CO_2 laser oscillators are often used as transmitters for coherent lidar applications. These oscillators suffer from intrapulse "chirp", or dynamic frequency shifting. If excessive, such chirp can limit the signal-to-noise of the lidar (by generating excess bandwidth), or limit the velocity resolution if the lidar is of the Doppler type. This paper describes a detailed numerical model that considers all known sources of intrapulse chirp. Some typical predictions of the model are shown, and simple design rules to minimize chirp are proposed.

INTRODUCTION

Pulsed CO_2 lasers are one important technology for application as coherent laser radar (or lidar) transmitters. Given today's technological resources, the CO_2 laser remains the tool of choice for coherent lidar applications. However, the performance of real-world coherent lidar systems is more often than not limited by unwanted intrapulse frequency sweeping ("chirp"). To understand and minimize intrapulse chirp in short-pulse TEA CO_2 laser oscillators is an essential ingredient of high-performance coherent lidar design.

There appears to be a well-accepted concensus within the community as to the physical origins of dynamic refraction and, hence, chirp.[1] This paper is an attempt to incorporate this existing understanding into a more accurate tool for the prediction of laser chirp.

Chirp is believed to result from dynamic changes of refractive index within the laser medium on time scales comparable to the laser pulse length. Probable causes of such index changes are discussed in the following section. An intracavity index change maps into a time-varying laser output frequency:

$$\delta\nu(t) = \nu_0 \frac{\ell}{L} \delta n(t) \qquad [1]$$

where $\delta\nu$ is the frequency shift ("chirp"), ν_0 is the laser frequency, ℓ is the gain medium length, L the total resonator length, and δn the index variation within the gain region.

The frequency change in the laser output can be viewed either as a drift in the longitudinal resonator mode frequency, or as a cumulative Doppler shift in the frequency of the trapped radiation in the resonator. Both pictures produce equivalent predictions for the relation between index change and chirp, as long as the index change is sufficiently slow. The condition defining "slow" changes is:

$$\ell \frac{\delta n(t)}{\delta t} \ll c \frac{\lambda_0}{L} \tag{2}$$

Here c is the speed of light and λ_0 is the operating wavelength, corresponding to ν_0.

Chirp Mechanisms

There are three distinct generally accepted causes of dynamic refractive index and, hence, laser chirp. These are **time-varying** electron density in the laser plasma, **time-varying** gas density because of a thermal expansion, and time variation of inversion density. Each of these three causes has a characteristic signature that makes **it** readily distinguishable from the others.

In most pulsed CO_2 lasers, the electron density is falling rapidly during the early part of the optical output pulse, which coincides with the trailing edge of the electrical excitation pulse. This effect causes a down chirp, which levels out as the electron density becomes small. The electron driven component is often called the "early" chirp. Its magnitude is typically of order 1 MHz.

After lasing begins, a radial thermal distribution develops due to optical extraction. Each extracted photon leaves behind a vibrationally excited CO_2 molecule, which is eventually converted to heat. There is a thermal maximum coinciding with the intensity maximum (usually on axis) of the laser mode. This thermal maximum drives a fluid dynamic expansion, which eventually results in a drop in gas density, hence, index near the center line of the resonator. An upchirp results with frequency increasing, typically, quadratically with time. This fluid dynamic effect is sometimes called the "late" chirp, because it increases quadratically or cubically with time, and becomes most evident late in the pulse. The magnitude of the late chirp can vary from 0.5 to greater than 5 MHz in typical CO_2 oscillators.

The final chirp component results from anomalous dispersion, due to the laser inversion. For typical CO_2 lasers systems, which operate near line center where the anomalous dispersion component goes through zero, this effect **can be ignored**. However, for certain applications, there may be externally imposed constraints forcing operation away from line center. For a given offset frequency, the magnitude of the anomalous dispersion component decreases monotonically throughout

the pulse, as the inversion is depleted. The sign of the inversion driven term changes on opposite sides of line center.

Estimation of Chirp Magnitude

Rough estimates of the plasma and anomalous dispersion contributions to chirp can be made by using the end point values of the driving terms, and the characteristic times over which they change. The fluid dynamic term is more difficult to estimate, since it is sensitive to very small changes in gas density, which in turn can vary wildly depending on the laser configuration.

Fortunately, the fluid dynamic component of chirp is amenable to a useful analytical model, if certain simplifying assumptions are made. Figure 1 shows the predictions of such a model, which treats the special case of Gaussian beams. The time behavior of the heat input is also treated in a very simplified fashion; the heat addition resulting from the extracted laser energy is presumed to be all deposited at the beginning of the pulse. The resultant predicted quadratic chirp can be described by a single coefficient, which is found to scale with a single parameter depending on the laser aperture (σ), longitudinal resonator fill factor (ℓ/L), the gas Gladstone-Dale coefficient (K) and ratio of specific heats (γ), and the laser energy (E_L). There is a particularly strong dependence on the tranverse dimension σ of the laser resonator. Larger apertures lead to lower chirp, since the thermal gradients are smaller in magnitude when spread over a larger area. As seen in Figure 1, there is good qualitative agreement between this scaling model and the measured performance of a number of dissimilar laser systems.

Detailed Chirp Model

While these rough estimates and scaling analyses are useful, they are insufficient to support detailed predictions of the complete time dependent output waveform of a given laser. Such predictions are often needed as input to a lidar system model, which will ultimately predict the performance of the complete lidar. Therefore, a detailed numerical model has been constructed to include all of the known chirp inducing mechanisms. Our goal was to arrive at the highest possible degree of quantitative accuracy within the resources available.

Figure 2 shows the structure of the resultant model. An existing laser kinetics model (upper left) serves as the point of departure. This model predicts laser output, given the geometry, gas mixture, and pump conditions. Internally, this model carries time dependent values for electron density and inversion density. Time dependent heating is modeled by applying a finite V-T relaxation rate to the lower state population which results from lasing. Because of the full rate

equation approach used, the correct time relationships are maintained between cause and effect throughout the kinetics model.

The electron density and inversion densities lead directly to index changes via the appropriate dispersion relations. The temperature change is used as the source term in a 2-D transient fluid solver, which predicts gas density. The gas density then is fed to the transient index calculation. The index calculation leads directly to a prediction of frequency, following Equation 1. More detailed mode modeling has been built into the structure of the model, but not yet implemented. The utility of better mode models is discussed below.

Figure 3 shows typical predictions of the chirp model. Only the operating pressure was changed between the two cases shown. Both frequency and intensity time histories are included in the figure. The frequency is displayed as the change in resonator mode relative to the pre-pump value. There is a large upchirp in the mode frequency during pumping, due to the rapid rise in electron density. This effect is responsible for the large offset from zero seen at the beginning of the frequency trace. If excessive, this effect can result in a failure of frequency selection in an injection locked system. In a hybrid system, the frequency scale used is realistic if the cw lasing frequency before pumping is treated as the zero reference.

The modeled case was 300 MHz above line center, to maximize the anomalous dispersion component. For positive offsets, the anomalous dispersion tends to cancel the other terms and slightly reduce the peak excursion in the frequency time history. This effect is most clearly visible at 0.5 atm, where anomalous dispersion causes the double minimum behavior seen in the frequency history.

The value of the detailed chirp model is most obvious in the lower pressure case, where the specifics of the time history substantially change the implications of the various chirp mechanisms. Lasing always lags the pump pulse, by an amount that increases at lower pressure. This lag increases by a few tenths of a microsecond as the pressure is decreased from 1 to 0.5 atm. While seeming minor, this additional lag is sufficient to drastically reduce the significance of the early chirp component at lower pressure. In contrast, the 1 atm case shows the highest rate of frequency change during the highest intensity part of the output pulse. The difference between these two cases, which results from a subtle difference of time relationships, cannot be readily predicted by simpler analyses of chirp behavior.

DIRECTIONS FOR FUTURE WORK

The results that have been shown have so far used an ad-hoc Gaussian intensity distribution as a model of the transverse resonator mode structure. In the presence of the saturation, or for unstable resonators, such a model is clearly not accurate. These details are important in defining the extraction-induced thermal gradients, which drive the fluid dynamic chirp component. Figure 4 shows an example of the detailed radial intensity distribution calculated for an unstable resonator equipped CO_2 transmitter, as recently built by Spectra Technology, Inc. (STI) for the National Oceanic and Atmospheric Administration. Clearly, there are very large small-scale gradients near the center of the resonator, where the laser frequency is in some sense determined. We believe that future chirp models should include such a resonator as one component so that the thermal gradients can be better modeled.

REFERENCES

1. Willetts, D.V., Harris, M.R.: Scaling Laws for the Intrapulse Frequency Stability of an Injection Mode Selected TEA CO_2 Laser. IEEE J. Quantum Electron. (USA), Vol. QE-19, No. 5, May 1983, pp. 810-14.

CHIRP COEFFICIENT, α MHz/μsec^2

10

1.0

0.1

0.01

p - 1 atm
GAUSSIAN BEAM

1983

1982

WILLETTS AND HARRIS

NOAA/UTRC
TRAILER LIDAR

p = 0.5 atm
GAUSSIAN BEAM

STI/NOAA
2 J, 0.5 atm

△ DESIGN POINT
☐ MEASUREMENT

0.01   0.1   1.0   10.0

SCALING PARAMETER, $\dfrac{(\gamma-1)\,\nu\,K}{2}\left(\dfrac{\ell}{L}\right)\dfrac{E_L}{\sigma^2}$, 10^{18} sec^{-3}
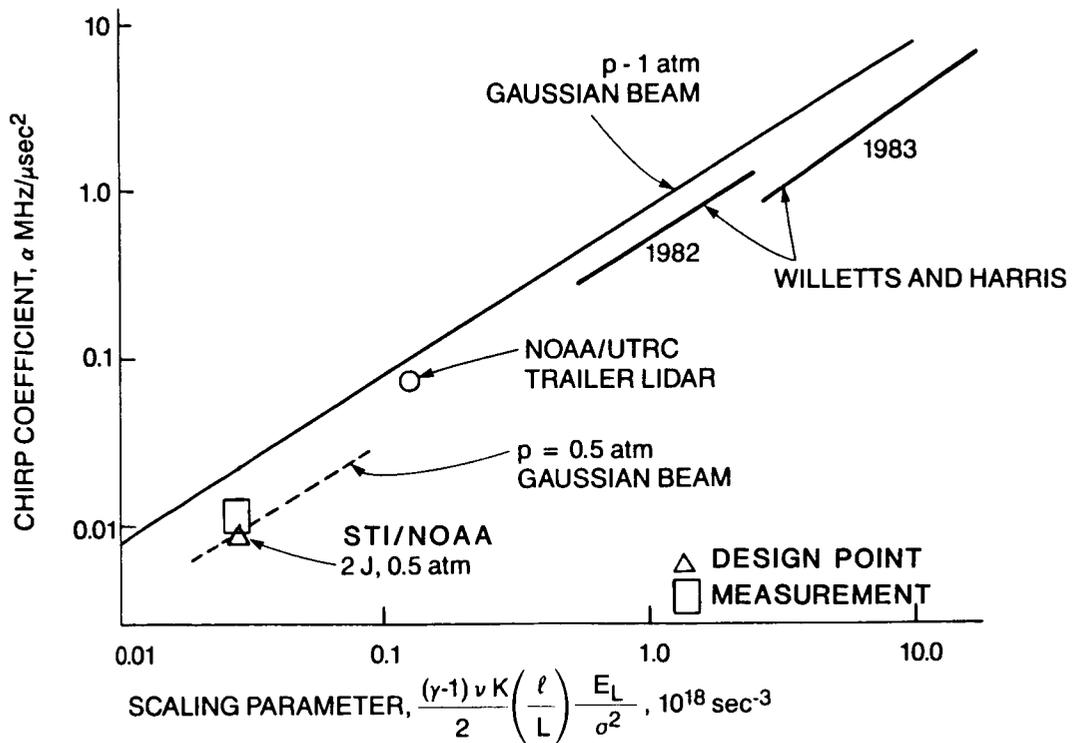
Figure 1.   Predictions of Fluid Dynamic Chirp Scaling Model

LASER
KINETICS

$T(t)$

2-D FLUID
SOLVER

$n_e(t)$
$(N_u-N_\ell)(t)$

$\rho(t)$

$I(r, \theta)$

INDEX
CALCULATION

MODE MODEL

———— = FUTURE
ENHANCEMENT

$\nu(t)$
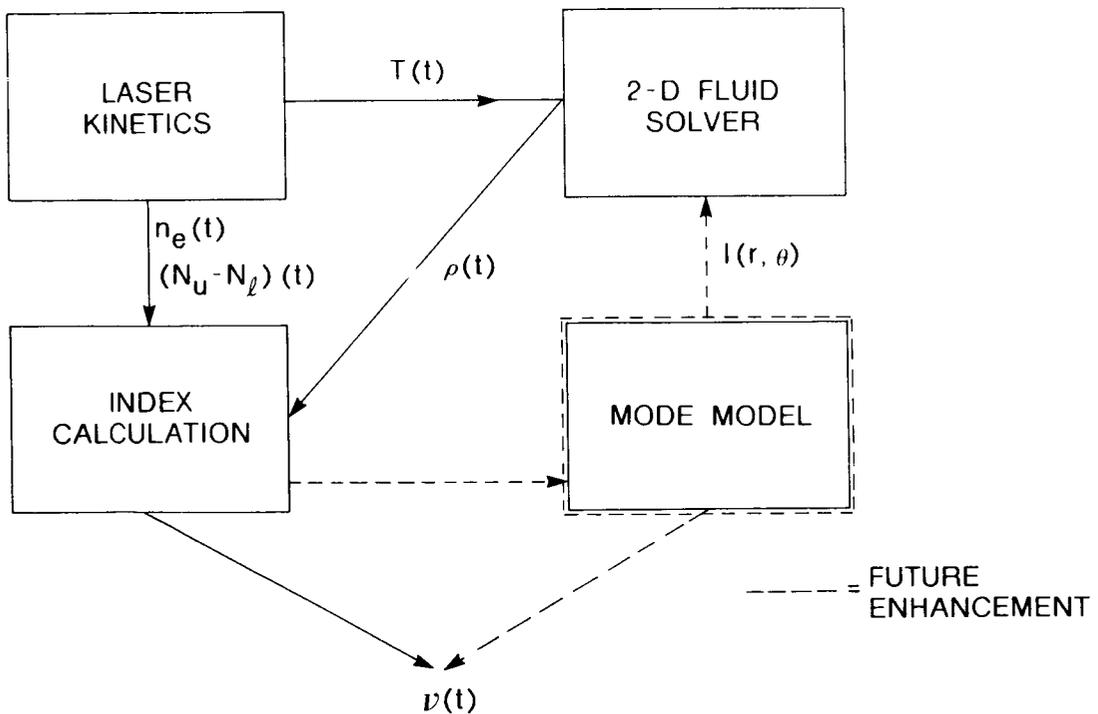
Figure 2.   Structure of Detailed Numerical Chirp Prediction Model

1.0 Atmosphere

(plot: Δν (MHz) vs TIME (μsec))
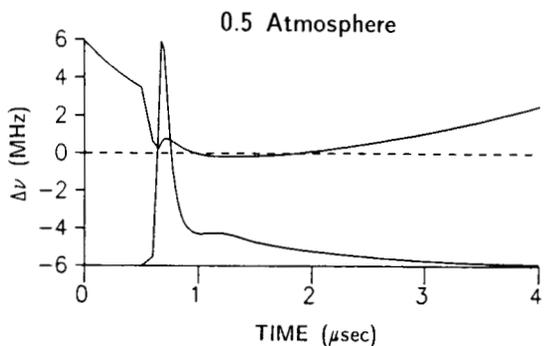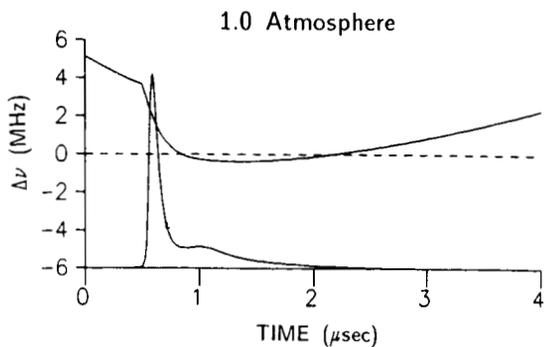
- Chirp (frequency shift) vs time overlaid on laser output intensity plot.

- Chirp scale was offset so that output spectrum peaked at $\Delta\nu = 0$.

0.5 Atmosphere

(plot: Δν (MHz) vs TIME (μsec))

- Injected frequency was at 300 MHz higher than line center (anomalous dispersion component was thus negative).

Figure 3. Sample Predictions of Chirp Model

FLAT - SPHERICAL
UNSTABLE RESONATOR
$M = 1.7$, $N_{eq} = 1.49$
$D_1 = 2.74$ cm
$D_2 = 3.70$ cm
$L = 3.50$ m

—— AT BACK MIRROR
––– 30 cm FROM BACK MIRROR
–·– TEM_{oo} MODE OF SEMI-CONFOCAL STABLE CAVITY
$\sigma = 0.31$ cm
······· LARGE APERTURE GAUSSIAN
$\sigma = 1.1$ cm

(plot: INTENSITY (ARBITRARY UNITS) vs RADIUS, cm)
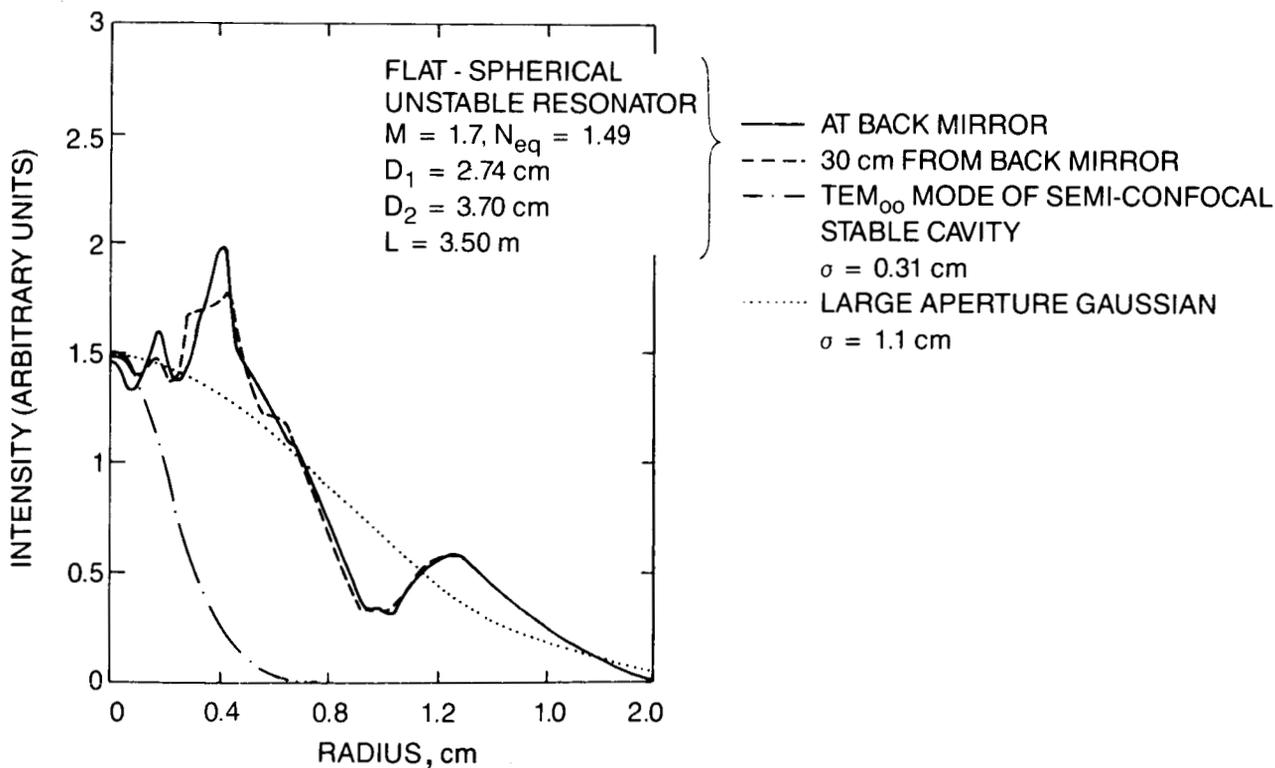
Figure 4. Calculated Intensity Distribution in Unstable Resonator